



# HHS Public Access

Author manuscript

*J Mol Biol.* Author manuscript; available in PMC 2021 November 10.

Published in final edited form as:

*J Mol Biol.* 2021 August 20; 433(17): 167104. doi:10.1016/j.jmb.2021.167104.

## Mapping Electromechanical Coupling Pathways in Voltage-Gated Ion Channels: Challenges and the Way Forward

**John Cowgill, Baron Chanda**

Department of Anesthesiology, Washington University, St. Louis, MO 63110, United States

Center for Investigations of Membrane Excitability Disorders (CIMED), Washington University, St. Louis, MO 63110, United States

### Abstract

Inter- and intra-molecular allosteric interactions underpin regulation of activity in a variety of biological macromolecules. In the voltage-gated ion channel superfamily, the conformational state of the voltage-sensing domain regulates the activity of the pore domain via such long-range allosteric interactions. Although the overall structure of these channels is conserved, allosteric interactions between voltage-sensor and pore varies quite dramatically between the members of this superfamily. Despite the progress in identifying key residues and structural interfaces involved in mediating electromechanical coupling, our understanding of the biophysical mechanisms remains limited. Emerging new structures of voltage-gated ion channels in various conformational states will provide a better three-dimensional view of the process but to conclusively establish a mechanism, we will also need to quantitate the energetic contribution of various structural elements to this process. Using rigorous unbiased metrics, we want to compare the efficiency of electromechanical coupling between various sub-families in order to gain a comprehensive understanding. Furthermore, quantitative understanding of the process will enable us to correctly parameterize computational approaches which will ultimately enable us to predict allosteric activation mechanisms from structures. In this review, we will outline the challenges and limitations of various experimental approaches to measure electromechanical coupling and highlight the best practices in the field.

### Keywords

voltage-sensing; allostery; linkage analysis; GIA; kinetic analysis

---

This is an open access article under the CC BY-NC-ND license (<http://creativecommons.org/licenses/by-nc-nd/4.0/>).

**Correspondence to Baron Chanda:** Department of Anesthesiology, Washington University, St. Louis, MO 63110, United States. [bchanda@wustl.edu](mailto:bchanda@wustl.edu) (*B. Chanda*).

CRediT authorship contribution statement

**John Cowgill:** Conceptualization, Writing - review & editing. **Baron Chanda:** Conceptualization, Writing - review & editing.

Declaration of Competing Interest

The authors declare that they have no known competing financial interests or personal relationships that could have appeared to influence the work reported in this paper.

## Introduction

Ion channels are highly specialized enzymes that catalyze the passage of ions across a hydrophobic barrier which is either the plasma membrane or an intracellular organellar membrane.<sup>1</sup> Most ion channels are involved in some form of cellular signaling and their activity is typically regulated by external stimuli. Some are activated by ligands such as cAMP<sup>2</sup> and calcium<sup>3</sup> while others also respond to physical stimuli such as voltage and mechanical stretch. Voltage-gated ion channels (VGICs) constitute an important superfamily of ion channels that are likely evolved by fusion of a specialized voltage-sensing module with pore module.<sup>4</sup> There are a number of ion channels whose activity is also regulated by voltage to varying extent even though they lack the voltage-sensing module<sup>5</sup> but in this review, we will limit our discussion to those that belong to the voltage-gated channel superfamily.

The channels within this superfamily share a common tetrameric architecture. Within a single subunit, the first four transmembrane (TM) helices come together as a four-helix bundle and constitute the voltage-sensing module (VSD). The most characteristic feature of VSD is the charged 4th TM helix which is also known as the S4 helix.<sup>6,7</sup> In a typical voltage-gated ion channel, every third residue in the S4 helix is positively charged and these charged residues are the primary sensors of transmembrane voltage.<sup>8–10</sup> The movement of this charged S4 helix in response to changes in membrane potential results in a series of conformational changes that culminate in either opening or closing of pore gates. This molecular process that couples voltage-sensor conformational state to pore activity has been sometimes referred to as electromechanical coupling and will be the main focus of this review.<sup>11,12</sup>

To characterize the biophysical mechanisms of electromechanical coupling, we need an understanding of both structure and dynamics. 3D structures of the channel in various conformational states enables us to readily formulate possible physical mechanisms which can then be thoroughly tested by experimental means.<sup>12</sup> Structures must be complemented by an understanding of the forces that drive these conformational changes. In electromechanical coupling, as in an allosteric network, we are interested in identifying how conformational energy flows from the stimulus sensing module to pore gates. In order to determine the contribution of various structural elements, we need reliable estimates of electromechanical coupling energy. With a well-defined metric in hand, it becomes possible to carry out systematic structure–function measurements to identify the interaction networks involved in transfer of energies and provide a comprehensive understanding of the physical mechanism.

## Standard Definition of Coupling

The thermodynamic underpinnings of electromechanical coupling are best illustrated by considering a simple allosteric system consisting of two elementary units, where one is the sensory module (voltage sensor) and the other is a catalytic module (pore).<sup>13,14</sup> Note that the sensory module has also been referred to as an effector domain elsewhere.<sup>15</sup> These two allosteric units are connected by at most four possible interactions that depend on the state of

these modules (Figure 1). Due to these state-dependent interactions, a change in the state of the voltage sensor alters the status of the pore. The functional output of such a system is the dose activity curve which is a function of the intrinsic equilibrium constants for each of the two modules as well as the strength of the coupling interactions between the two allosteric units.

In a two-element allosteric model system described above, there are four types of coupling interactions between elements: resting VSD-closed pore ( $\theta_{RC}$ ), resting VSD-open pore ( $\theta_{RO}$ ), activated VSD-closed pore ( $\theta_{AC}$ ), and activated VSD-open pore ( $\theta_{AO}$ ). In addition, each individual element is governed by an intrinsic equilibrium constant ( $K_{VSD}$  and  $K_{Pore}$ ). This gives a total of six thermodynamic parameters which define the system at equilibrium. In an experimental setting, one can extract at most three non-dependent parameters from an allosteric model consisting of two allosteric units. As shown previously, these two models can be reconciled by normalization.<sup>16,17</sup> This normalization makes it evident that the experimentally measured equilibrium constants associated with voltage-sensor activation ( $K_V$ ) and pore opening ( $K_P$ ) in an intact system are not the true intrinsic equilibrium constants. In principle, one can measure the true equilibrium constants by independently measuring the spontaneous activity of each of the particles in the absence of the other interacting particles, but this is rarely possible in practice.

In the normalized version, one can use an inclusive coupling term,  $\theta$  to describe the strength of interaction between the two allosteric particles. In most channels, electromechanical coupling ties the activation of the voltage sensor to pore opening. Thus, coupling is a measure of the strength of the interactions in the RC and AO states (termed 'like' states) relative to the RO and AC states ('unlike' states). The coupling term  $\theta$ , is expressed as a ratio between the like and unlike state-dependent interaction terms (Figure 1). When  $\theta$  is greater than 1, the model exhibits positive cooperativity whereas when  $\theta$  is less than 1, it corresponds to negative cooperativity.

Alternatively, coupling can be viewed as the change in the observed equilibrium constant of one element when the state of the other element is fixed in each state. For example, the  $\theta$  term is equal to the ratio of the observed equilibrium constant for pore opening when the voltage sensor is in the activated state ( $K_P^A$ ) relative to the resting state ( $K_P^R$ , Figure 1(D)). This is also equal to the ratio of voltage sensor activation when the pore is open ( $K_V^O$ ) versus closed ( $K_V^C$ ). As a result, the effects of coupling interaction in the system are bidirectional, the activation of the voltage sensor increases the favorability of pore opening by the same margin which pore opening increases the favorability of voltage sensor activation.

## Quantitative Methods for Measuring Coupling Energies

High-resolution structures of channels in various conformational states make it possible to conceptualize models of channel gating and highlight the possible pathways for propagation of allosteric interactions.<sup>12</sup> In order to validate a mechanism, however, it is necessary to demonstrate that particular structural elements are able to transmit the underlying force to drive these conformational changes. Here, we will discuss the various

approaches that have been used to determine the allosteric interaction pathways involved in electromechanical coupling. We should point out that most studies would benefit from use of multiple approaches to mitigate the limitations of a single approach in order to build a more complete understanding of electromechanical coupling in a channel.

### Integrated measures of allosteric coupling

**Allosteric linkage analysis.**—Allosteric linkage analysis was first introduced by Jeffries Wyman to understand the cooperative binding of oxygen to hemoglobin. For an allosteric system, the Hill transformation of dose–response will result in a curve that approaches linearity at extremely high and low doses.<sup>18</sup> The difference in the y-intercept of the limiting asymptotes is directly proportional to the normalized coupling energy. This fundamental relationship can be extended to a system where the allosteric propagation involves  $N$  intermediate particles, as in a real protein.<sup>16</sup> In the case of EM coupling, the Hill transformation of relative open probability *versus* voltage curves ( $\ln[P_o/(1 - P_o)]$  *versus*  $V$ ) can be utilized to calculate the coupling energy. This transformation generates a characteristic logistic curve where the slopes of the two limiting asymptotes at high and low potentials will become identical and the difference in their y-intercepts is called  $\chi$ -value, which is directly proportional to the normalized coupling energy of the system (Figure 2(A)).

In our view, if an allosteric system is amenable to linkage analysis, it should be the first approach that should be considered because it can directly resolve questions regarding the effect of mutations on binding vis-à-vis gating. The other advantage of this method is that it provides us an integrated measure of coupling strength between the two allosteric units as seen in Figure 2.<sup>16,19</sup> Furthermore, the difference in the y-intercepts of limiting asymptotes is purely interaction terms and does not contain any of the intrinsic equilibrium constant terms even if one considers the all parameter allosteric model (see Chowdhury and Chanda<sup>16</sup> for derivations). Finally, in addition to quantifying the effects on the strength of the coupling energy, the Hill transform plots can also help determine whether the mutations affect resting state interactions or the activated state interactions.<sup>20</sup>

Nonetheless, the need to accurately determine  $P_o$  at extreme potentials have hindered more widespread application of linkage analysis. As is evident from Figure 2(A), as the strength of allosteric coupling between the two domains increase, the magnitude of separation between the two limiting asymptotes increase which means that one has to accurately measure small values of  $P_o$  to define the lower asymptote. In the Shaker potassium channel, for instance, it has not been possible to measure the coupling strength between the voltage-sensor and the pore because the  $P_o$  values do not reach the asymptotic limit even when the  $P_o$  is  $10^{-7}$ .<sup>10</sup> At an open probability this low, the channel spends nearly 3 hours in the closed state for every millisecond in the open state, so it is difficult to observe enough opening events to determine the  $P_o$  accurately. Furthermore, in a channel that approximates the strict or obligate coupling regime, the asymptotic limit will never be reached. The other limitation of this approach is that it is not clear how one treats the subconductance states that are sometimes observed in single channel recordings. Typically, one should consider this part of the open channel but this might introduce some ambiguity in the measurements.

This approach has provided insight on the voltage-dependent gating in  $K_{ir}2.1$ <sup>21</sup> and to probe the calcium- and temperature-dependent activation of the archeal MthK channel.<sup>22</sup> One promising approach that circumvents some of the limitation of measuring low  $P_o$  values is to use a mutant with increased basal open probability which will move the limiting asymptote into the experimentally accessible range. This approach has been used by Auerbach lab<sup>23</sup> and Goldschen-Ohm lab<sup>24</sup> to probe coupling in pentameric ligand-gated receptors but, to the best of our knowledge, has not been used in the VGIC field. Note that this modification provides a relative estimate of the contributions of various residues to electromechanical coupling.

**Kinetic analysis of allosteric models.**—The methods detailed above utilize equilibrium channel gating properties to elucidate thermodynamic parameters of coupling. Over the years, electrophysiologists have successfully built explicit kinetic models to describe the gating behavior of many ion channels especially for key model systems. This list includes the models for voltage-gated ion channels<sup>25–27</sup> and ligand-gated ion channels.<sup>28,29</sup>

In a typical electrophysiological experiment, there is a wealth of information carried in the non-equilibrium properties of channel gating. Kinetic modeling can harness both the equilibrium and non-equilibrium gating properties to extract a much more thorough understanding of channel function. In kinetic modeling, users define models of channels with various states and interconnectivities that can be used to simulate or fit experimentally observed channel properties. This is done through numerical solution of the transition matrix (Q-matrix) for a given model to solve for the time- and stimulus-dependent state occupancies.<sup>30</sup> With a detailed model in hand, it is possible to find experimental conditions to extract the allosteric coupling term.

This approach has been primarily used to measure the allosteric coupling between voltage-sensing pathway and pore gating in the BK channels.<sup>27,31–33</sup> We note that this approach also necessitates measurement of voltage-independent channel openings at very high and low voltages, essentially the same requirement as in allosteric linkage analysis. As noted earlier, it has not been possible to obtain an estimate for coupling strength for the Shaker potassium channel despite the existence of a well-constrained kinetic models for more than two decades.<sup>10,25</sup> Therefore, while the detailed models provide rich information about the kinetic barriers to gating processes, it does not circumvent the limitations of allosteric linkage analysis.

**Gating in conformationally locked channels.**—In principle, allosteric linkage analysis can also be carried out by measuring  $P_o$  values from channels where the voltage-sensor is chemically locked in either activated or resting conformations as opposed to applying strong voltages to reach the limiting conditions (Figure 2(C)). Furthermore, the same allosteric coupling term can also be estimated by locking the pore in one conformation and measuring the excess voltage (force) required to drive the voltage-sensor to non-permissive conformation (Figure 2(D)).<sup>19</sup> To get a complete estimate of the electromechanical coupling strength, these measurements have to be carried out in both locked open and locked close states.

A version of this approach was first used to identify mutants that disrupt coupling between the lidocaine bound open pore and domain III voltage-sensor.<sup>20</sup> Haddad and Blunck also used a similar approach to identify mutants that disrupt coupling between open pore stabilized in relaxed conformation and the voltage-sensing domain.<sup>34</sup> In both these cases, there is some ambiguity as to the nature of possible structure of open pore given that it is either blocked or relaxed. Yellen and coworkers overcame this limitation by locking the pore in either closed or open state using cysteine crossbridge.<sup>35</sup> They were able to measure the coupling energy by probing the difference in the Q-V curve when the pore is locked open or locked close.

There are couple of assumptions inherent to this technique that must be carefully considered. The primary one being that the locked conformation corresponds to the native open and closed states. Additionally, the treatment that locks the state of one domain should not directly influence the equilibrium properties of the other domain. For example, a toxin that binds to the resting voltage sensor may also interact with the pore domain through a pathway that is distinct from the normal coupling pathway.

Despite these limitations, this approach to measuring coupling energy is convenient because it gives a direct readout of the normalized coupling energy ( $\Theta$ ) between the two domains. Furthermore, as structural biology approaches become prevalent, it has become possible to rationally engineer mutations and treatments that lock the conformational state of the voltage sensor and/or pore for numerous channel types. These provide convenient starting points for mutagenic studies to identify pathways for electromechanical coupling in channels like HCN, two-pore channels, and voltage-gated sodium channels.<sup>36–38</sup>

### Discretized measures of allosteric coupling

Double mutant cycle was first used by Alan Fersht and his colleagues to probe interactions between residues in the active site of tyrosyl t-RNA synthetase.<sup>39</sup> It has its roots in the Hammett equation that was formulated to estimate interaction between aromatic ring substituents.<sup>40</sup> Briefly, this method involves comparing the free-energies associated with double substituents to that of sum of free-energies from corresponding single substituents. If the difference is non-zero, then then this value corresponds to interaction energy between the two sites.

The Mackinnon group introduced this approach to the ion channel community by using it to measure interaction energies between sites on a channel and peptide toxin.<sup>41</sup> In the modified method, the associated free-energy is obtained by measuring conductance-voltage curves of the various mutants. Assuming that the channel exists only in two states, these curves are fit to a Boltzmann function with only two free parameters, charge ( $z$ ) and  $V_{1/2}$  which can then be used to calculate the free-energy of channel opening. Since this type of double mutant cycle analysis is based on functional measurements, it has been also referred to as functional mutant cycle analysis.

The functional mutant cycle analysis (FMC) has been frequently used to characterize a variety of interactions including allosteric interactions. However, the application of this approach to measure allosteric interactions is fundamentally flawed. When the channel

exists in more than two states, conductance-voltage curves no longer represent the free-energy of activation and therefore is not a thermodynamic state function.<sup>19,42,43</sup> By definition, this requirement excludes any allosteric system which must exist at least in four possible states. Chowdhury *et al.* have shown previously that even in a defined model system, the non-additivity observed in FMC analysis has no bearing to the true interaction energies.<sup>43</sup> Our view is that the use of functional mutant cycle to estimate allosteric interactions has no theoretical basis and should not be used in the field.

The fundamental shortcoming of FMC can be overcome if one uses the gating charge *versus* voltage ( $Q-V$ ) curves instead of  $G-V$  curves.<sup>19,43</sup> The free energy of channel activation can be computed from the  $Q-V$  curve using median voltage analysis and it requires experimental determination of the gating charge per channel ( $Q_{\text{Max}}$ ) and the median voltage ( $V_{\text{M}}$ ). The  $V_{\text{M}}$  is computed directly from the normalized  $Q-V$  curve as the integrand of the curve relative to the y-axis. Unlike  $V_{1/2}$  of  $G-V$  curve,  $V_{\text{M}}$  of  $Q-V$  curve is a thermodynamic state function and depends only on the energy difference between the initial and final state and not the number of intermediates states or the complexity of the underlying model. Double mutant cycle analysis based on  $Q-V$  measurements, which is also referred to as Generalized Interaction energy analysis (GIA), is an excellent alternative to FMC to quantify the contribution of interacting residues to channel activation without the limiting assumptions inherent to FMC.<sup>44</sup>

Despite the strength of the GIA approach, there are few key considerations that must be taken into account when interpreting these measurements. First of all, GIA is measure of the change in interaction energy relative to one state. The lack of non-additivity does not mean that these sites do not interact but only that their interaction does not change upon channel gating. Second, the discretized interaction energy may not correlate with total coupling energy between the two allosteric units. It is conceivable, for instance, that some positive interactions are countered by negative interactions between the two domains. Therefore, GIA should be used to measure interaction strengths between sites in two allosteric domains only when there is other evidence to suggest that these sites are likely to contribute to allosteric coupling.

## Semi-Quantitative Approaches for Mapping Coupling Pathways

The quantitative methods described above provide means to systematically characterize the electromechanical coupling pathways in a channel but more coarse-grained techniques have been widely used to map the possible pathways of allosteric energy transduction. Below, we provide a list of these semi-quantitative methods that have greatly shaped our understanding of electromechanical coupling in the VGIC superfamily.

### Chimeragenesis and other protein engineering techniques

Despite the similarities in sequence and architecture within the VGIC superfamily, the gating phenotypes, and thus electromechanical coupling mechanisms are quite diverse. Most channels are voltage-dependent, but some are voltage-independent; most channels open upon depolarization but some open upon hyperpolarization; some channels undergo inactivation while others are non-inactivating, just to name a few common phenotypic

differences. Chimeragenesis takes advantage of this functional diversity in homologous channels by swapping regions or residues between channels with differing function in an attempt to localize structural elements underlying phenotypic differences. This approach is often useful as a first pass to localize regions or domains that are critical for electromechanical coupling.

One of the main pitfalls of chimeragenesis is the relatively low success rate of producing functional chimeras. The low success rate is often attributed to structural perturbations that lead to misfolding or mis-trafficking due to use of incompatible junction points. Another concern is that domains may not retain the same fold/function in chimeras as they do in the parent constructs. The influx of three-dimensional structures for most channel types in the VGIC superfamily has enabled structure-guided chimeragenesis, which greatly improves the ability to identify compatible junction points based on structural alignments. Despite the limitations, chimeragenesis has historically been one of the most important techniques guiding our understanding of sensing, gating, and coupling mechanisms in ion channels.<sup>45,46</sup>

Lörinczi *et al.* introduced a new approach to examine the necessity of covalent linkage between the VSD and pore by recombinantly co-expressing these two domains in the same cell from separate transcripts.<sup>47</sup> Surprisingly, these split or demi channels can still assemble and traffic to the plasma membrane and in some cases even retain similar gating properties to the wild-type parent channel. This approach has been used to demonstrate that many members of the cyclic nucleotide-gated clade of channels retain voltage sensitivity without a covalent connection between VSD and pore.<sup>47,48</sup> It is important to note that the inability to generate functional demi channels for a given parent construct does not prove that a covalent linkage is necessary for gating since it cannot be ruled out that structural perturbations impeded trafficking or folding. Furthermore, the isolated domains may adopt an alternative fold or acquire a new function that complicates interpretation.<sup>49</sup>

### Voltage-clamp fluorometry

The strength of electromechanical coupling determines how tightly pore gating correlates with voltage sensor movement. Therefore, independently measuring voltage sensor movement and pore opening is an effective way of examining the coupling between these two domains. While gating currents are the most direct measure of voltage sensor movement (see GIA above), this approach is often arduous and not practical for many channel types. An alternative is to spectroscopically track conformational changes in the voltage sensor using voltage clamp fluorometry (VCF).<sup>50</sup> VCF enables detection of conformational changes in the voltage sensor via a fluorescent probe while simultaneously monitoring pore opening through macroscopic current recordings.

Once a suitable probe site is identified for VSD movement, mutations can be introduced to disrupt suspected coupling pathways between the voltage sensor and pore. Mutation of residues involved in coupling will produce a net shift in the fluorescence-voltage ( $F-V$ ) curve relative to the  $P_o-V$  curve.<sup>20,34,51</sup> However, the interpretation that these shifts are only due to mutations that affect allosteric coupling rather than intrinsic pore opening or voltage-sensor movement requires more careful consideration. Muroi *et al.* showed that only when the mutations affect both like state interactions does this cause an opposite shift in



the two curves.<sup>20</sup> Thus, the criteria of opposing shifts in  $F-V$  and  $P_0-V$  curves has been widely used in the field, they likely capture only a fraction of possible allosteric coupling interactions.

The other consideration for using  $F-V$  curve as a measure of the voltage-sensor movement is that the probe may detect conformational changes unrelated to the voltage-sensor movement. In some instances, conformational changes in the voltage sensor may not result in an environmental change but those in neighboring regions of the channel may be responsible for most of the fluorescence change. Nevertheless, the ability to simultaneously monitor conformational changes and channel function with sub-millisecond resolution makes VCF a useful tool for identifying residues involved in electromechanical coupling, especially if combined with kinetic modeling.

## Current Understanding of Electromechanical Coupling in VGICs

Since the cloning of voltage-gated ion channels in the 80s, studies using the above approaches have fueled an ever-improving understanding of channel gating in the VGIC superfamily. Excellent reviews have been written in the field which provide a detailed historical perspective of electromechanical coupling.<sup>52,53</sup> In the sections below, we will summarize some of the key advances that have shaped our current view of electromechanical coupling with a goal to highlight the current gaps in our understanding. While semi-quantitative approaches have been widely employed in these studies, use of quantitative techniques has remained limited.

### Canonical view of electromechanical coupling

Sequences and functional studies of VGICs clearly identified the role of S4 helix in voltage sensing. Likewise, the role of the intracellular S6 bundle crossing in channel had been uncovered by cysteine accessibility studies and the structure of KcsA.<sup>54,55</sup> It was not clear from these studies, however, how voltage sensor movement controlled the state of the pore. McCormick *et al.* originally suggested the S4-S5 linker plays an important role coupling VSD movement to pore gating on the basis that mutations decreased the slope of relative open-probability *versus* voltage curves.<sup>56</sup> While numerous alternative mechanisms can alter the slope of the Po-V curve, Schoppa and Sigworth confirmed this proposed role in electromechanical coupling for one position in the S4-S5 linker.<sup>26</sup> They used gating current recordings paired with open probability measurements and extensive kinetic modeling to show that the voltage dependence of charge movement and channel opening were shifted in opposing directions by the mutation, a clear sign of disrupted coupling. Subsequent studies on the putative S4-S5 linker of the human ether-a-go-go related gene (hERG) channel showed that the D540K mutation dramatically disrupted pore closing at hyperpolarized potentials beyond resting potential indicating that this residue is involved in voltage-sensor pore coupling.<sup>57</sup>

The S4-S5 linker is an intuitive site for electromechanical coupling as it is the covalent linkage between the VSD and PD. In a series of classical experiments, Lu *et al.* showed that the chimeras which included the pore of voltage-insensitive KcsA channel can become voltage-sensitive when linked to the voltage-sensing domain of the Shaker potassium

channel.<sup>45,46</sup> They found that the voltage-sensitivity was retained as long as the S4-S5 linker and the interface of S6 was maintained providing evidence that this region may have all the necessary molecular machinery to couple voltage-sensor movements to pore opening.

In the following years, extensive mutagenesis in Shaker and other VGICs focused on the S4-S5 linker and C-terminus of S6. These studies identified specific positions in these regions that were critical in electromechanical coupling as evidenced by increases in the basal open probability, increased separation in the voltage dependence of charge movement and pore gating, or changes to the sigmoidicity/cooperativity of channel activation. The Sanguinetti group even showed that the hyperpolarization-dependent opening of the hERG D540K could be abrogated through a subsequent neutralization or charge reversal at the C-terminus of S6 (R665), suggesting a direct electrostatic interaction of these regions.<sup>58</sup>

The first structures for Shaker-type channels showed that the S4-S5 helix forms a short helix running parallel to the membrane plane.<sup>12,59</sup> This is due to the domain-swapped nature of the transmembrane domains of these channels, where the VSD of one subunit is nearest to the pore domain of an adjacent subunit. As a result, the S4-S5 linker is in direct contact with the C-terminus of S6 of the same subunit in the open state of the pore. This arrangement would produce a steric clash between the S4-S5 linker and the C-terminus of S6 when S4 moves downward upon hyperpolarization, pushing the gate closed (Figure 3).<sup>12</sup> Molecular dynamics simulations of channel deactivation from the Kv1.2/2.1 chimera structure agreed with this proposed gating model.<sup>60</sup> Additionally, numerous structures of voltage-gated sodium channels and two-pore channels with voltage sensors trapped in the resting state have supported this canonical gating mechanism in other channel types.

### Non-canonical coupling pathways

From the structure of the Kv1.2/2.1 chimera, Soler-Llavina *et al.* noted the presence of extensive *intersubunit* contacts between the transmembrane regions of S4 and S5.<sup>61</sup> Using extensive mutagenesis along this interface paired with gating and macroscopic current recordings, they identified several mutations along the S4-facing surface of S5 which severely disrupted electromechanical coupling. Many of these positions on S5 are in contact with the sites of the ILT mutations (V369I, I372L, and S376T) on S4 that were known to uncouple voltage sensor movement from pore gating.<sup>62</sup> Fernandez *et al.* used the GIA approach detailed earlier to quantify the contribution of these and other interactions along the intersubunit interface between S4 and S5.<sup>63</sup> These measurements provide compelling evidence that the interactions mediated by residues in transmembrane helices at the interface of VSD and pore domain also contribute significantly to electromechanical coupling in prototypical voltage-gated ion channels.

The notion that non-canonical pathways are central to electromechanical coupling has gained more ground in recent years in part driven by new structures that show that many channels within the VGIC superfamily lack a well-defined S4-S5 linker domain.<sup>64–67</sup> Cui and coworkers have recently shown that in KCNQ channels the pathway for electromechanical coupling is dependent on the state of the voltage-sensor. KCNQ channels are unique because these channels can access an open state even when the voltage-sensor is in an intermediate position.<sup>51,68,69</sup> The canonical pathway mediates the coupling between

the intermediate voltage-sensor and the pore whereas when the voltage-sensor is fully activated, the open pore conformation is stabilized by a non-canonical pathway.

Using the unnatural fluorescent amino acid ANAP, Kalstrup and Blunck describe a similar two-step electromechanical coupling in the Shaker channel, with the first transition driving pore opening while the second drives C-type inactivation.<sup>70</sup> The Bezanilla lab has shown critical interactions between S4 and the S5 helix of an adjacent subunit critical for coupling voltage sensor movement to C-type inactivation.<sup>71,72</sup> Thus, the canonical and non-canonical coupling pathways may have evolved concurrently to confer more precise tuning of the channel response to membrane potential.

**Non-domain swapped channels.**—Many of the early studies on the members of the KCNH family (including EAG, ERG, and ELK channels) mirrored studies detailed above on the more distantly related members of the voltage-gated potassium channel superfamily. Mutagenic studies suggested interactions between residues in the putative S4-S5 linker with S6 C-terminus played an important role in electromechanical coupling in these channel types.<sup>57,73</sup> The first indication that something was significantly different in these channels came from studies of split or “demi” channels lacking covalent linkage between the VSD and pore as exemplified by studies on EAG and hERG channels.<sup>74</sup> Moreover, much of the sequence corresponding to the S4-S5 linker could be removed in these demi-channels without perturbing voltage gating which clearly demonstrates that the canonical VSD-pore coupling cannot account for gating in these channels.

The cryoEM structure of EAG solved soon after highlighted a unique structural difference in the arrangement of the VSD and PD (Figure 4).<sup>67</sup> Unlike any other VGIC structure solved at the time, the EAG transmembrane domains adopted a non-domain swapped fold, meaning that the VSD was nearest to the PD of its own subunit. As a result, the S4-S5 linker was formed by just a small loop segment and further demonstrated that the mechanical lever model of gating was not compatible with structure of these channels.

Another interesting feature of the EAG and hERG structures is the wide separation between the S4 and S5 transmembrane segments. As these channels both gate in the absence of the S4-S5 linker segment, one would expect tight interactions in the transmembrane interfaces between the VSD and pore underlying electromechanical coupling in these channels.<sup>66,67</sup> It is possible that tighter interactions form along this interface during deactivation of the voltage sensor, stabilizing the closed state of the pore. This would be consistent with the proposal that the closed state of the pore is unstable and requires specific interactions with the VSD to remain closed.<sup>75</sup> The supposed intrinsic stability of the open state of the hERG pore has been attributed to a lack of the PVP hinge at the end of S6 observed in other channels.<sup>75,76</sup>

The short S4-S5 linker in these non-domain swapped channels likely restricts the vertical S4 movement during activation more so than the domain-swapped counterparts. The nature of the conformational change associated with voltage sensing is not well understood in these channels and, as we will discuss in the next section, may be distinct from the canonical vertical movement expected in VGICs.

**Hyperpolarization-activated channels.**—While nearly all channels in the VGIC superfamily activate upon membrane depolarization, a small subset of channels in the CNBD family activate on hyperpolarization. These include the mammalian HCN channel and the plant channels KAT and AKT. Similar to other members of the VGIC superfamily, these hyperpolarization-activated channels possess positive charges on the S4 helix that sense changes in the electric field across the membrane.<sup>77</sup> Movement of these gating charges is transmitted to the PD where dilation and constriction of a hydrophobic gate opens and closes the pore.<sup>78</sup> As the voltage sensing and pore gating mechanisms in these channels are shared with the depolarization-activated members of the VGIC superfamily, the prevailing hypothesis for the inverted voltage-dependence of HCN channel gating has been an inversion of the VSD-PD coupling.

Early mutagenesis experiments showed evidence for interactions between the S4-S5 linker and the C-terminus of S6, as was expected given the canonical mechanism for coupling that was developing at the time.<sup>73</sup> Kwan *et al.* used high affinity metal bridges to demonstrate state-dependent interactions in the closed and open states between the S4-S5 linker and C-linker and C-terminus of S6.<sup>79</sup> These metal bridges locked the channel in either the closed or open state depending on the interacting pair that was bridged. The Yellen group later used these locked open and closed channels to measure the coupling energy between the VSD and PD, which revealed that the coupling energy in spHCN channels is much lower than that of canonical VGICs such as Shaker.<sup>35</sup>

The cryoEM structure of HCN1 showed that, like the related EAG and CNG channels solved previously, HCN channels adopt a non-domain swapped architecture.<sup>65</sup> The extended length of the S4 helix of HCN1 compared to all previously known VGICs enabled new interactions between the VSD and C-linker region. Additionally, the VSD of HCN1 packs directly against the PD in the closed state structure, providing a tighter interface for VSD-PD coupling compared to other channel types.

Flynn and Zagotta demonstrated that spHCN demi-channels also retain voltage sensitivity.<sup>48</sup> They posited that the HCN pore is more stable in the open state and that interactions between the voltage sensor and the S5 N-terminus maintain the channel in the closed state under depolarizing conditions. In support of this idea, chimeras between HCN and EAG with a mismatched S4-S5 interface reopen upon depolarization and this opening can be obscured through preservation of the HCN specific interactions between S4 and S5.<sup>80</sup> Furthermore, spHCN voltage dependence is completely inverted through the double mutation W355N (S4 C-terminus) and N370W (S5 N-terminus).<sup>81</sup> This critical role of S4-S5 interactions in closed-state stabilization resembles proposals for hERG gating, albeit with inverted voltage dependence.

Molecular dynamics simulations<sup>82</sup> and the cryoEM structure of the HCN1 voltage sensor in an activated conformation<sup>37</sup> revealed a unique voltage sensor movement underlying channel activation. Upon downward movement of the gating charges, the S4 helix breaks at S272 into two sub-helices; the N-terminal S4 remains perpendicular to the membrane plane while the C-terminal S4 bends parallel to the membrane (Figure 4(B)). Despite voltage sensor activation in both the structure and simulation, the pore remained in the

closed conformation. Thus, further studies are needed to understand how this unique voltage sensor movement drives channel opening in HCN channels. Nevertheless, it is clear that the helix-breaking transition of the HCN voltage sensor is a critical determinant for inverted gating as hydrophobic substitutions of the hinge point S272 can completely invert gating polarity in HCN-EAG chimeras.<sup>82</sup>

The unique movement of the S4 helix is not the sole determinant of inverted gating polarity of the channel, as chimeras with EAG containing just the S3b-S4 segment of HCN retain depolarization-activation of the EAG parent.<sup>80</sup> Other elements from HCN are required to rescue hyperpolarization-dependent gating in these chimeras including residues near the gate on S6 previously implicated by the Sanguinetti group as well as the HCN C-terminus.<sup>73</sup> While the C-terminus of HCN1 can be fully removed with minimal perturbation to hyperpolarization activation, removing the HCN C-terminus dramatically favors the depolarization-activation pathway in HCN-EAG chimeras. This profound influence of the C-terminus on channel gating polarity in these chimeras is not well understood and warrants further study.

## Dynamic Coupling

It is becoming abundantly evident that electromechanical coupling is dynamically regulated by a variety of cofactors. These include lipid modulators and auxiliary subunits which alter the interactions between the voltage sensor and pore. This type of modulation opens the door for pharmacological manipulation of channel activity with compounds selectively targeting these interfaces. Below, we will highlight several emerging examples of dynamic regulation of electromechanical coupling.

### Lipids in electromechanical coupling

One of the most prevalent and well characterized examples of lipid modulation of electromechanical coupling in the VGIC superfamily is the secondary messenger phosphatidyl inositol 4,5 bisphosphate (PIP<sub>2</sub>). Numerous channels are regulated by PIP<sub>2</sub> including Shaker-type, hERG, EAG, KCNQ, and HCN.<sup>83–88</sup> In the case of KCNQ channels, PIP<sub>2</sub> is required to couple VSD movement to pore opening.<sup>89,90</sup> Structures of KCNQ with and without PIP<sub>2</sub> show that binding at the VSD-pore interface induces a large conformational change at the C-terminus of S6 responsible for opening the channel.<sup>91</sup> The effects of PIP<sub>2</sub> on coupling in other channel types are more complex. Shaker-type, EAG, and sPHCN channels have all been shown to have dual effects from PIP<sub>2</sub> suggesting multiple binding sites.<sup>83,85–88</sup> For example, in Shaker-type channels, PIP<sub>2</sub> shifts the voltage-dependence of activation to more positive potentials, indicating the channel is harder to open.<sup>86</sup> Yet, the maximal current amplitude through the channel is increased, as if PIP<sub>2</sub> is an agonist.

Other lipid modulators are thought to play a role in regulation of channel activity including sterols, ceramides, and polyunsaturated fatty acids. Overall, the roles of lipids in electromechanical coupling are generally not well understood and will likely be aided by elucidation of lipids bound to channels in emerging cryoEM structures in near-native environments.

### Auxiliary subunits in electromechanical coupling

In addition to lipids, auxiliary subunits can play a critical role in modulating the physiological channel activity. These effects can be the result of altered electromechanical coupling or via alternative mechanisms such as altered surface charge or channel trafficking.

In KCNQ channels, the KCNE1 beta subunit alters coupling to prevent channel opening from the intermediate state of the VSD that is observed in channels expressed without this accessory subunit.<sup>92,93</sup> Crosslinking studies and a recent cryoEM structure have identified a binding site for the related KCNE3 subunit right at the VSD-Pore interface, directly opposed to the PIP<sub>2</sub> binding site.<sup>91,94</sup> This is consistent with the altered electromechanical coupling induced by coexpression with the KCNE1 subunit.

### Pharmacological modulation of electromechanical coupling

The existence of lipid and auxiliary protein modulators of EM coupling points to druggable target sites which can be harnessed to modulate channel activity by altering VSD-pore coupling. Jara-Oseguera *et al.* have shown that ruthenium complexes such as the carbon-monoxide releasing molecule2 (CORM-2) weaken EM coupling in Shaker-type (K<sub>V</sub>1) and K<sub>V</sub>2.1 channels.<sup>95</sup> Based on mutagenesis and molecular docking, these compounds likely bind near the S4-S5 linker, a critical site for EM coupling in these channels.

Liu *et al.* used similarity-based *in silico* screening and molecular docking of a library of compounds to identify CP1 as a novel compound which could target the PIP<sub>2</sub> binding site in KCNQ channels.<sup>96</sup> They showed that CP1 rescues channel rundown induced by PIP<sub>2</sub> depletion and could rescue drug-induced action potential prolongation in guinea pig ventricular cardiomyocytes. Interestingly, CP1 had no measurable effect on several other channels with known PIP<sub>2</sub>-sensitivity, highlighting the potential of this strategy to identify new modulators with high specificity.<sup>96</sup>

### Concluding Remarks

Understanding the mechanisms of electromechanical coupling has been one of the central questions in the field of voltage-gated ion channels. High-resolution structures of the channels in various conformations enabled us to envision detailed physical models of channel gating and voltage-transduction<sup>12,36,38</sup> Functional and spectroscopic measurements have helped us identify the key residues or regions that are involved in electromechanical coupling (Figure 5).<sup>61,63</sup> Given the diversity of functional behavior and the interaction of EM coupling pathways with other regulatory pathways, it is unsurprising that many questions remain outstanding. For instance, early experiments showed that compatible interfaces were necessary for EM coupling<sup>46</sup> but subsequent studies showed that coupling can be achieved even in absence of conserved interface.<sup>97</sup> In absence of quantitative estimates, it is not clear whether EM coupling is equally efficient in both these sets of chimeras. More broadly, it remains unclear which of the two pathways –canonical vis-a-vis non-canonical- contribute most to the electromechanical coupling and whether these differ between the domain swapped structure and non-domain swapped structures. Developments of robust and facile quantitative methods to characterize electromechanical coupling will

allow us to compare allosteric pathways across the VGIC superfamily and formulate general principles of electromechanical coupling.

An emerging frontier in the field is the use of computational approaches to understand the mechanisms of channel gating and activation (see accompanying review by Elbahnsi and Delemotte). We are entering an era in which computational advances will play an increasingly important role in development and rational design of new drugs.<sup>98</sup> For instance, the protein folding appears to have been “solved” by state-of-the art machine learning algorithms.<sup>99</sup> The development and success of the new generation of empirical models is dependent on availability of robust standardized datasets which we are currently lacking. In the meantime, computational methods will continue to guide experimental studies to identify and map key interaction pathways.

It is also becoming increasingly evident that extrinsic factors such as lipids and small molecule compounds also play an important role in regulating electromechanical coupling. By modulating the strength of EM coupling, these compounds can act as partial agonists of voltage-gating response. We anticipate systematic investigations of mechanism of action of these modulators will further our understanding of electromechanical coupling and help design new class of therapeutics.

## Acknowledgements

We thank National Institutes of Health (NS-116850, NS-101723, NS-081293, GM131662), McDonnell Center for Neuroscience, CIMED and Department of Anesthesiology for research support. We thank the Prof. Lucie Delemotte, Prof. Jianmin Cui, Prof. Sandipan Chowdhury and the anonymous reviewers for their thoughtful feedback.

## References

1. Hille B, (2001). Ion channels of excitable membranes. Sinauer, Sunderland, Mass.
2. Craven KB, Zagotta WN, (2006). CNG and HCN channels: two peas, one pod. *Annu. Rev. Physiol*, 68, 375–401. [PubMed: 16460277]
3. Giraldez T, Rothberg BS, (2017). Understanding the conformational motions of RCK gating rings. *J. Gen. Physiol*, 149, 431–441. [PubMed: 28246116]
4. Swartz KJ, (2008). Sensing voltage across lipid membranes. *Nature*, 456, 891–897. [PubMed: 19092925]
5. Moran Y, Barzilai MG, Liebeskind BJ, Zakon HH, (2015). Evolution of voltage-gated ion channels at the emergence of Metazoa. *J. Exp. Biol*, 218, 515–525. [PubMed: 25696815]
6. Catterall WA, (2010). Ion channel voltage sensors: structure, function, and pathophysiology. *Neuron*, 67, 915–928. [PubMed: 20869590]
7. Bezanilla F, (2008). How membrane proteins sense voltage. *Nature Rev. Mol. Cell Biol*, 9, 323–332. [PubMed: 18354422]
8. Aggarwal SK, MacKinnon R, (1996). Contribution of the S4 segment to gating charge in the Shaker K<sup>+</sup> channel. *Neuron*, 16, 1169–1177. [PubMed: 8663993]
9. Seoh SA, Sigg D, Papazian DM, Bezanilla F, (1996). Voltage-sensing residues in the S2 and S4 segments of the Shaker K<sup>+</sup> channel. *Neuron*, 16, 1159–1167. [PubMed: 8663992]
10. Islas LD, Sigworth FJ, (1999). Voltage sensitivity and gating charge in Shaker and Shab family potassium channels. *J. Gen. Physiol*, 114, 723–742. [PubMed: 10539976]
11. Yellen G, (2002). The voltage-gated potassium channels and their relatives. *Nature*, 419, 35–42. [PubMed: 12214225]

12. Long SB, Campbell EB, MacKinnon R, (2005). Voltage sensor of Kv1.2: structural basis of electromechanical coupling. *Science*, 309, 903–908. [PubMed: 16002579]
13. Leff P, (1995). The two-state model of receptor activation. *Trends Pharmacol. Sci*, 16, 89–97. [PubMed: 7540781]
14. Monod J, Wyman J, Changeux J-P, (1965). On the nature of allosteric transitions: a plausible model. *J. Mol. Biol*, 12, 88–118. [PubMed: 14343300]
15. Motlagh HN, Wrabl JO, Li J, Hilser VJ, (2014). The ensemble nature of allostery. *Nature*, 508, 331–339. [PubMed: 24740064]
16. Chowdhury S, Chanda B, (2010). Deconstructing thermodynamic parameters of a coupled system from site-specific observables. *PNAS*, 107, 18856–18861. [PubMed: 20944067]
17. Chowdhury S, Chanda B, (2012). Thermodynamics of electromechanical coupling in voltage-gated ion channels. *J. Gen. Physiol*, 140, 613–623. [PubMed: 23183697]
18. Wyman J, (1967). Allosteric linkage. *J. Am. Chem. Soc*, 89, 2202–3000.
19. Sigg D, (2012). A linkage analysis toolkit for studying allosteric networks in ion channels Linkage analysis in ion channels. *J. Gen. Physiol*, 141, 29–60. [PubMed: 23250867]
20. Muroi Y, Arcisio-Miranda M, Chowdhury S, Chanda B, (2010). Molecular determinants of coupling between the domain III voltage sensor and pore of a sodium channel. *Nature Struct. Mol. Biol*, 17 230–U14. [PubMed: 20118934]
21. Sigg DM, Chang H-K, Shieh R-C, (2018). Linkage analysis reveals allosteric coupling in Kir2.1 channels. *J. Gen. Physiol*, 150, 1541–1553. [PubMed: 30327330]
22. Jiang Y, Idikuda V, Chowdhury S, Chanda B, (2020). Activation of the archaeal ion channel MthK is exquisitely regulated by temperature. *eLife*, 9, e59055. [PubMed: 33274718]
23. Purohit P, Auerbach A, (2009). Unliganded gating of acetylcholine receptor channels. *PNAS*, 106, 115–120. [PubMed: 19114650]
24. Nors JW, Gupta S, Goldschen-Ohm MP, (2021). A critical residue in the  $\alpha$ 1M2–M3 linker regulating mammalian GABAA receptor pore gating by diazepam. *eLife*, 10, e64400. [PubMed: 33591271]
25. Zagotta WN, Hoshi T, Aldrich RW, (1994). Shaker potassium channel gating. III: Evaluation of kinetic models for activation. *J. Gen. Physiol*, 103, 321–362. [PubMed: 8189208]
26. Schoppa NE, Sigworth FJ, (1998). Activation of Shaker potassium channels. III. An activation gating model for wild-type and V2 mutant channels. *J. Gen. Physiol*, 111, 313–342. [PubMed: 9450946]
27. Horrigan FT, Aldrich RW, (2002). Coupling between voltage sensor activation, Ca<sup>2+</sup> binding and channel opening in large conductance (BK) potassium channels. *J. Gen. Physiol*, 120, 267–305. [PubMed: 12198087]
28. Lape R, Colquhoun D, Sivilotti LG, (2008). On the nature of partial agonism in the nicotinic receptor superfamily. *Nature*, 454, 722–727. [PubMed: 18633353]
29. Nayak TK, Auerbach A, (2017). Cyclic activation of endplate acetylcholine receptors. *Proc. Natl. Acad. Sci. USA*, 114, 11914–11919. [PubMed: 29078356]
30. Colquhoun D, Lape R, (2012). Allosteric coupling in ligand-gated ion channels. *J. Gen. Physiol*, 140, 599–612. [PubMed: 23183696]
31. Horrigan FT, (2012). Conformational coupling in BK potassium channels. *J. Gen. Physiol*, 140, 625–634. [PubMed: 23183698]
32. Horrigan FT, Aldrich RW, (1999). Allosteric voltage gating of potassium channels II: Mslo channel gating charge movement in the absence of Ca<sup>2+</sup>. *J. Gen. Physiol*, 114, 305–336. [PubMed: 10436004]
33. Horrigan FT, Cui J, Aldrich RW, (1999). Allosteric voltage gating of potassium channels I. Mslo ionic currents in the absence of Ca(2+). *J. Gen. Physiol*, 114, 277–304. [PubMed: 10436003]
34. Haddad GA, Blunck R, (2011). Mode shift of the voltage sensors in Shaker K<sup>+</sup> channels is caused by energetic coupling to the pore domain. *J. Gen. Physiol*, 137, 455–472. [PubMed: 21518834]
35. Ryu S, Yellen G, (2012). Charge movement in gating-locked HCN channels reveals weak coupling of voltage sensors and gate. *J. Gen. Physiol*, 140, 469–479. [PubMed: 23071265]



36. Guo J, Zeng W, Chen Q, Lee C, Chen L, Yang Y, et al. , (2016). Structure of the voltage-gated two-pore channel TPC1 from *Arabidopsis thaliana*. *Nature*, 531, 196–201. [PubMed: 26689363]
37. Lee C-H, MacKinnon R, (2019). Voltage sensor movements during hyperpolarization in the HCN channel. *Cell*, 179 1582–9.e7. [PubMed: 31787376]
38. Wisedchaisri G, Tonggu L, McCord E, Gamal El-Din TM, Wang L, Zheng N, et al. , (2019). Resting-state structure and gating mechanism of a voltage-gated sodium channel. *Cell*, 178 993–1003.e12. [PubMed: 31353218]
39. Carter PJ, Winter G, Wilkinson AJ, Fersht AR, (1984). The use of double mutants to detect structural changes in the active site of the tyrosyl-tRNA synthetase (*Bacillus stearothermophilus*). *Cell*, 38, 835–840. [PubMed: 6488318]
40. Hammett LP, (1937). The effect of structure upon the reactions of organic compounds. Benzene derivatives. *J. Am. Chem. Soc*, 59, 96–103.
41. Hidalgo P, MacKinnon R, (1995). Revealing the architecture of a K<sup>+</sup> channel pore through mutant cycles with a peptide inhibitor. *Science*, 268, 307–310. [PubMed: 7716527]
42. Bezanilla F, Villalba-Galea CA, (2013). The gating charge should not be estimated by fitting a two-state model to a Q-V curve. *J. Gen. Physiol*, 142, 575–578. [PubMed: 24218396]
43. Chowdhury S, Chanda B, (2012). Estimating the voltage-dependent free energy change of ion channels using the median voltage for activation. *J. Gen. Physiol*, 139, 3–17. [PubMed: 22155736]
44. Chowdhury S, Haehnel BM, Chanda B, (2014). Generalized interaction energy analysis of intersubunit linkage in shaker potassium channels. *Biophys. J*, 106 742A–A.
45. Lu Z, Klem AM, Ramu Y, (2001). Ion conduction pore is conserved among potassium channels. *Nature*, 413, 809–813. [PubMed: 11677598]
46. Lu Z, Klem AM, Ramu Y, (2002). Coupling between voltage sensors and activation gate in voltage-gated K<sup>+</sup> channels. *J. Gen. Physiol*, 120, 663–676. [PubMed: 12407078]
47. Lőrinczi É, Gómez-Posada JC, de la Peña P, Tomczak AP, Fernández-Trillo J, Leipscher U, et al. , (2015). Voltage-dependent gating of KCNH potassium channels lacking a covalent link between voltage-sensing and pore domains. *Nature Commun*, 6, 6672. [PubMed: 25818916]
48. Flynn GE, Zagotta WN, (2018). Insights into the molecular mechanism for hyperpolarization-dependent activation of HCN channels. *Proc Natl Acad Sci USA*, 115 E8086–e95. [PubMed: 30076228]
49. Zhao J, Blunck R, (2016). The isolated voltage sensing domain of the Shaker potassium channel forms a voltage-gated cation channel. *Elife*, 5
50. Mannuzzu LM, Moronne MM, Isacoff EY, (1996). Direct physical measure of conformational rearrangement underlying potassium channel gating. *Science*, 271, 213–216. [PubMed: 8539623]
51. Hou P, Kang PW, Kongmeneck AD, Yang N-D, Liu Y, Shi J, et al. , (2020). Two-stage electro-mechanical coupling of a KV channel in voltage-dependent activation. *Nature Commun*, 11, 676. [PubMed: 32015334]
52. Blunck R, Batulan Z, (2012). Mechanism of electromechanical coupling in voltage-gated potassium channels. *Front. Pharmacol*, 3
53. Vardanyan V, Pongs O, (2012). Coupling of voltage-sensors to the channel pore: a comparative view. *Front. Pharmacol*, 3
54. Doyle DA, Cabral JM, Pfuetzner RA, Kuo A, Gulbis JM, Cohen SL, et al. , (1998). The structure of the potassium channel: molecular basis of K<sup>+</sup> conduction and selectivity. *Science*, 280, 69–77. [PubMed: 9525859]
55. Liu Y, Holmgren M, Jurman ME, Yellen G, (1997). Gated access to the pore of a voltage-dependent K<sup>+</sup> channel. *Neuron*, 19, 175–184. [PubMed: 9247273]
56. McCormack K, Tanouye MA, Iverson LE, Lin JW, Ramaswami M, McCormack T, et al. , (1991). A role for hydrophobic residues in the voltage-dependent gating of Shaker K<sup>+</sup> channels. *PNAS*, 88, 2931–2935. [PubMed: 2011602]
57. Sanguinetti MC, Xu QP, (1999). Mutations of the S4–S5 linker alter activation properties of HERG potassium channels expressed in *Xenopus* oocytes. *J. Physiol*, 514, 667–675. [PubMed: 9882738]

58. Tristani-Firouzi M, Chen J, Sanguinetti MC, (2002). Interactions between S4–S5 linker and S6 transmembrane domain modulate gating of HERG K<sup>+</sup> channels. *J. Biol. Chem*, 277, 18994–19000. [PubMed: 11864984]
59. Long SB, Campbell EB, MacKinnon R, (2005). Crystal structure of a mammalian voltage-dependent Shaker family K<sup>+</sup> channel. *Science*, 309, 897–903. [PubMed: 16002581]
60. Jensen MØ, Jogini V, Borhani DW, Leffler AE, Dror RO, Shaw DE, (2012). Mechanism of voltage gating in potassium channels. *Science*, 336, 229–233. [PubMed: 22499946]
61. Soler-Llavina GJ, Chang T-H, Swartz KJ, (2006). Functional Interactions at the interface between voltage-sensing and pore domains in the Shaker Kv channel. *Neuron*, 52, 623–634. [PubMed: 17114047]
62. Ledwell JL, Aldrich RW, (1999). Mutations in the S4 region isolate the final voltage-dependent cooperative step in potassium channel activation. *J. Gen. Physiol*, 113, 389–414. [PubMed: 10051516]
63. Fernandez-Marino AI, Harpole TJ, Oelstrom K, Delemotte L, Chanda B, (2018). Gating interaction maps reveal a noncanonical electromechanical coupling mode in the Shaker K<sup>+</sup> channel. *Nature Struct. Mol. Biol*, 25 320–+. [PubMed: 29581567]
64. Hite RK, MacKinnon R, (2017). Structural titration of Slo2.2, a Na<sup>+</sup>-dependent K<sup>+</sup> channel. *Cell*, 168 390–9.e11. [PubMed: 28111072]
65. Lee C-H, MacKinnon R, (2017). Structures of the human HCN1 hyperpolarization-activated channel. *Cell*, 168 111–20.e11. [PubMed: 28086084]
66. Wang W, MacKinnon R, (2017). Cryo-EM structure of the open human ether-à-go-go-related K<sup>+</sup> channel hERG. *Cell*, 169 422–30.e10. [PubMed: 28431243]
67. Whicher JR, MacKinnon R, (2016). Structure of the voltage-gated K<sup>+</sup> channel Eag1 reveals an alternative voltage sensing mechanism. *Science*, 353, 664–669. [PubMed: 27516594]
68. Hou P, Eldstrom J, Shi J, Zhong L, McFarland K, Gao Y, et al. , (2017). Inactivation of KCNQ1 potassium channels reveals dynamic coupling between voltage sensing and pore opening. *Nature Commun*, 8, 1730. [PubMed: 29167462]
69. Zaydman MA, Kasimova MA, McFarland K, Beller Z, Hou P, Kinser HE, et al. , (2014). Domain-domain interactions determine the gating, permeation, pharmacology, and subunit modulation of the IKs ion channel. *Elife*, 3, e03606 [PubMed: 25535795]
70. Kalstrup T, Blunck R, (2018). S4–S5 linker movement during activation and inactivation in voltage-gated K<sup>+</sup> channels. *Proc. Natl. Acad. Sci*, 115 E6751–E9. [PubMed: 29959207]
71. Bassetto CAZ, Carvalho-de-Souza JL, Bezanilla F, (2021). Molecular basis for functional connectivity between the voltage sensor and the selectivity filter gate in Shaker K<sup>+</sup> channels. *Elife*, 10, 18.
72. Carvalho-de-Souza JL, Bezanilla F, (2019). Noncanonical mechanism of voltage sensor coupling to pore revealed by tandem dimers of Shaker. *Nature Commun*, 10, 12. [PubMed: 30602727]
73. Decher N, Chen J, Sanguinetti MC, (2004). Voltage-dependent gating of hyperpolarization-activated, cyclic nucleotide-gated pacemaker channels: molecular coupling between the S4–S5 and C-linkers. *J. Biol. Chem*, 279, 13859–13865. [PubMed: 14726518]
74. de la Peña P, Domínguez P, Barros F, (2018). Gating mechanism of Kv11.1 (hERG) K(+) channels without covalent connection between voltage sensor and pore domains. *Pflugers Arch*, 470, 517–536. [PubMed: 29270671]
75. Wynia-Smith SL, Gillian-Daniel AL, Satyshur KA, Robertson GA, (2008). hERG gating microdomains defined by S6 mutagenesis and molecular modeling. *J. Gen. Physiol*, 132, 507–520. [PubMed: 18955593]
76. Thouta S, Sokolov S, Abe Y, Clark Sheldon J, Cheng Yen M, Claydon Tom W., (2014). Proline scan of the hERG channel S6 Helix reveals the location of the intracellular pore gate. *Biophys. J*, 106, 1057–1069. [PubMed: 24606930]
77. Männikkö R, Elinder F, Larsson HP, (2002). Voltage-sensing mechanism is conserved among ion channels gated by opposite voltages. *Nature*, 419, 837–841. [PubMed: 12397358]
78. Rothberg BS, Shin KS, Phale PS, Yellen G, (2002). Voltage-controlled gating at the intracellular entrance to a hyperpolarization-activated cation channel. *J. Gen. Physiol*, 119, 83–91. [PubMed: 11773240]

79. Kwan DCH, Prole DL, Yellen G, (2012). Structural changes during HCN channel gating defined by high affinity metal bridges. *J. Gen. Physiol*, 140, 279–291. [PubMed: 22930802]
80. Cowgill J, Klenchin VA, Alvarez-Baron C, Tewari D, Blair A, Chanda B, (2019). Bipolar switching by HCN voltage sensor underlies hyperpolarization activation. *PNAS*, 116, 670–678. [PubMed: 30587580]
81. Ramentol R, Perez ME, Larsson HP, (2020). Gating mechanism of hyperpolarization-activated HCN pacemaker channels. *Nature Commun*, 11, 1419. [PubMed: 32184399]
82. Kasimova MA, Tewari D, Cowgill JB, Ursuleaz WC, Lin JL, Delemotte L, et al. . (2019). Helix breaking transition in the S4 of HCN channel is critical for hyperpolarization-dependent gating. *eLife*, 8, e53400. [PubMed: 31774399]
83. Bian J, Cui J, McDonald TV, (2001). HERG K(+) channel activity is regulated by changes in phosphatidyl inositol 4,5-bisphosphate. *Circ. Res*, 89, 1168–1176. [PubMed: 11739282]
84. Zhang H, Craciun LC, Mirshahi T, Rohács T, Lopes CM, Jin T, et al. . (2003). PIP(2) activates KCNQ channels, and its hydrolysis underlies receptor-mediated inhibition of M currents. *Neuron*, 37, 963–975. [PubMed: 12670425]
85. Flynn GE, Zagotta WN, (2011). Molecular mechanism underlying phosphatidylinositol 4,5-bisphosphate-induced inhibition of SpIH channels. *J. Biol. Chem*, 286, 15535–15542. [PubMed: 21383006]
86. Abderemane-Ali F, Es-Salah-Lamoureux Z, Delemotte L, Kasimova MA, Labro AJ, Snyders DJ, et al. . (2012). Dual effect of phosphatidylinositol (4,5)-bisphosphate PIP(2) on Shaker K(+) [corrected] channels. *J. Biol. Chem*, 287, 36158–36167. [PubMed: 22932893]
87. Kruse M, Hille B, (2013). The phosphoinositide sensitivity of the KV channel family. *Channels*, 7, 530–536. [PubMed: 23907203]
88. Delgado-Ramírez M, López-Izquierdo A, Rodríguez-Menchaca AA, (2018). Dual regulation of hEAG1 channels by phosphatidylinositol 4,5-bisphosphate. *Biochem. Biophys. Res. Commun*, 503, 2531–2535. [PubMed: 30208521]
89. Kim RY, Pless SA, Kurata HT, (2017). PIP2 mediates functional coupling and pharmacology of neuronal KCNQ channels. *Proc. Natl. Acad. Sci. USA*, 114 E9702–e11. [PubMed: 29078287]
90. Zaydman MA, Silva JR, Delaloye K, Li Y, Liang H, Larsson HP, et al. . (2013). Kv7.1 ion channels require a lipid to couple voltage sensing to pore opening. *PNAS*, 110, 13180–13185. [PubMed: 23861489]
91. Sun J, MacKinnon R, (2020). Structural basis of human KCNQ1 modulation and gating. *Cell*, 180 340–7.e9. [PubMed: 31883792]
92. Barro-Soria R, Ramentol R, Liin SI, Perez ME, Kass RS, Larsson HP, (2017). KCNE1 and KCNE3 modulate KCNQ1 channels by affecting different gating transitions. *Proc. Natl. Acad. Sci. USA*, 114 E7367–e76. [PubMed: 28808020]
93. Hou P, Shi J, White KM, Gao Y, Cui J, (2019). ML277 specifically enhances the fully activated open state of KCNQ1 by modulating VSD-pore coupling. *Elife*, 8
94. Westhoff M, Murray CI, Eldstrom J, Fedida D, (2017). Photo-cross-linking of I(Ks) demonstrates state-dependent interactions between KCNE1 and KCNQ1. *Biophys. J*, 113, 415–425. [PubMed: 28746852]
95. Jara-Oseguera A, Ishida IG, Rangel-Yescas GE, Espinosa-Jalapa N, Pérez-Guzmán JA, Elías-Viñas D, et al. . (2011). Uncoupling charge movement from channel opening in voltage-gated potassium channels by ruthenium complexes. *J. Biol. Chem*, 286, 16414–16425. [PubMed: 21454671]
96. Liu Y, Xu X, Gao J, Naffaa MM, Liang H, Shi J, et al. . (2020). A PIP2 substitute mediates voltage sensor-pore coupling in KCNQ activation. *Commun. Biol*, 3, 385. [PubMed: 32678288]
97. Arrigoni C, Schroeder I, Romani G, Van Etten JL, Thiel G, Moroni A, (2013). The voltage-sensing domain of a phosphatase gates the pore of a potassium channel. *J. Gen. Physiol*, 141, 389–395. [PubMed: 23440279]
98. Silvera Ejneby M, Gromova A, Ottosson NE, Borg S, Estrada-Mondragon A, Yazdi S, et al. . (2021). Resin-acid derivatives bind to multiple sites on the voltage-sensor domain of the Shaker potassium channel. *J. Gen. Physiol*, 153

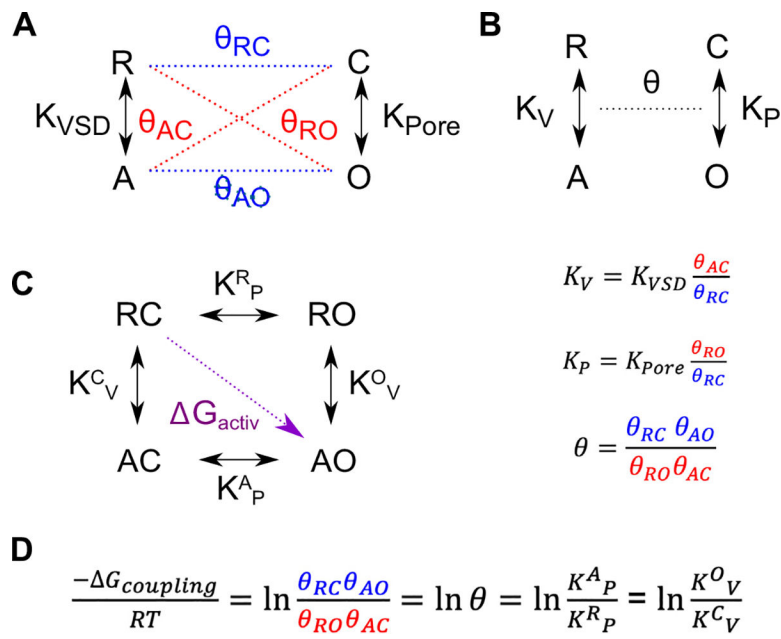
99. Senior AW, Evans R, Jumper J, Kirkpatrick J, Sifre L, Green T, et al. , (2020). Improved protein structure prediction using potentials from deep learning. *Nature*, 577, 706–710. [PubMed: 31942072]

Author Manuscript

Author Manuscript

Author Manuscript

Author Manuscript

**Figure 1.**

A. Model of a simple two-state VSD (left) coupled to a two-state pore domain (right). The VSD and PD are governed by intrinsic equilibrium constants while the two systems are coupled by state-dependent interactions. Interactions between ‘like’ states are shown in blue while interactions between unlike states are shown in red. B. Normalized allosteric model corresponding to the experimentally observable parameters of the model in A. The relationships between the parameters of the normalized and non-normalized models are shown below. C. Macrostates and connectivity of the allosteric system depicted in A-B. D. Equations relating the coupling energy to the various model parameters depicted in A-C.

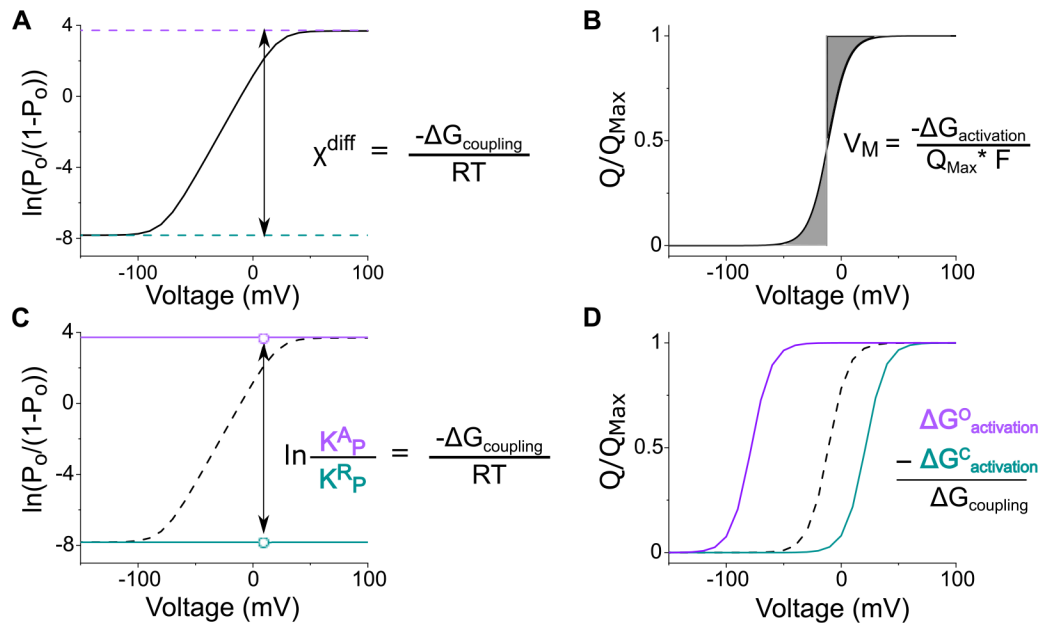


**Figure 2.**

A. Example measurement of coupling energy using X-value analysis. Black line represents theoretical experimental data while the colored dashed lines represent linear fits to the asymptotes. Coupling energy is computed from the difference in y-intercept of the two linear fits ( $X^{\text{diff}}$ ) from the inset equation. B. Example calculation of the free energy of channel activation from Q-V curve using median voltage analysis. Median voltage represents the potential where the two shaded regions are equal in area and is related to the free energy of activation by the equation shown. C. Calculation of the coupling energy using measurements of open probability in a channel with the VSD locked in the activated (purple) and resting (aqua) states. Open circles represent the Hill transformation of the open probability measured for the two conformationally locked systems and the coupling energy can be computed from these values according to the equation shown. D: Calculation of coupling energy using measurement of Q-V curves for channels locked in the open (purple) or closed (aqua) state. Coupling energy represents the difference in activation energy computed using median voltage analysis as shown in B.

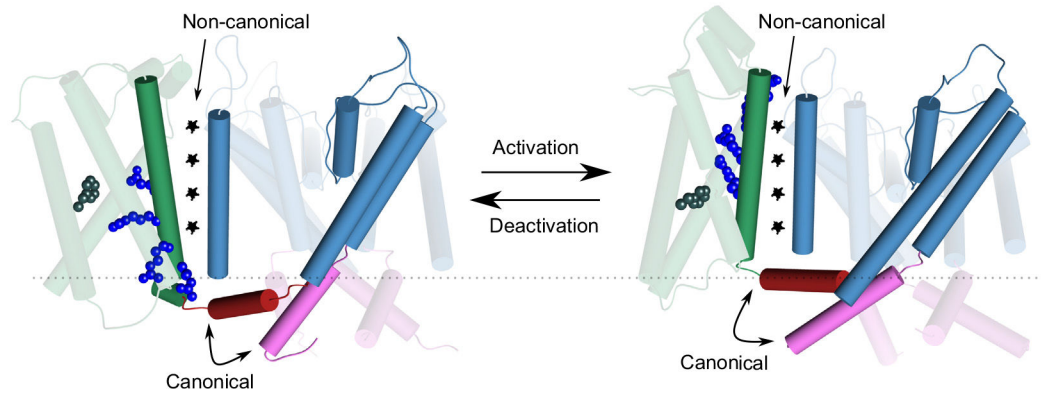


**Figure 3.**

Comparison of the resting structure of the Kv1.2/2.1 chimera from molecular dynamics simulations (left) to the activated-state crystal structure (right). The canonical intrasubunit coupling interface between the S4-S5 linker and S6 is highlighted as well as the non-canonical intersubunit coupling interface in the transmembrane regions of S4 and S5. The VSD is shown in green with the gating charges and charge transfer center highlighted in slate gray. The S4-S5 linker is shown in red and the C-terminus of S6 is shown in pink. The pore domain is colored blue. Only one VSD is shown for clarity with the dashed line representing the position of the S4-S5 linker in the activated state for comparison.

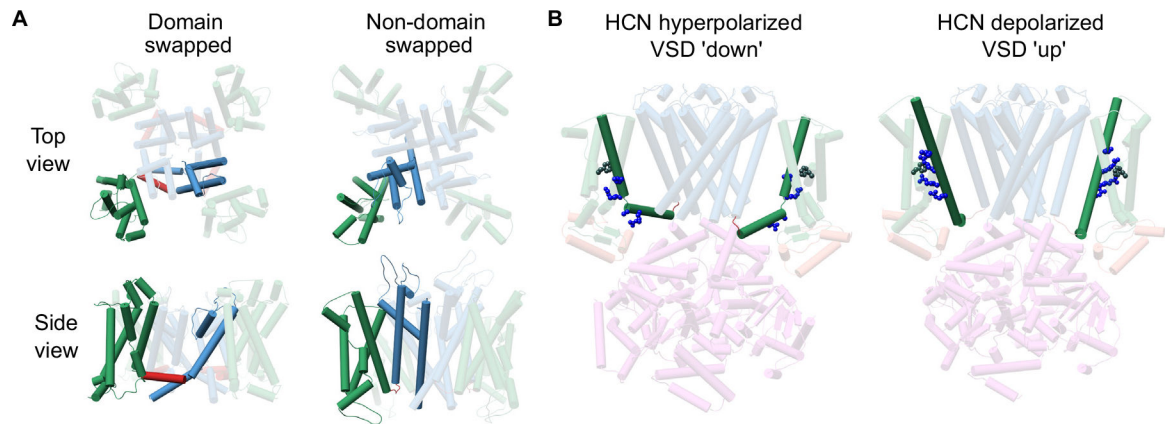


**Figure 4.**

A: Comparison of the architecture of domain-swapped channels (left, represented by Kv1.2/2.1 chimera) with non-domain swapped channels (right, represented by EAG). Top view is looking down through the central axis of the pore into the cell while side view is viewed from the membrane plane with the extracellular side of the channel facing up. The VSD is colored in green, the S4-S5 linker is colored in red, and the pore is colored in blue with one subunit highlighted for clarity. B. Non-canonical voltage sensor movement of HCN channel activation. Left represents the down state cryoEM structure obtained by mercury crosslinking while the up state represents the original construct. Upon downward movement, the S4 helix (highlighted in green) breaks into two helices, with one bending nearly parallel to the membrane plane.



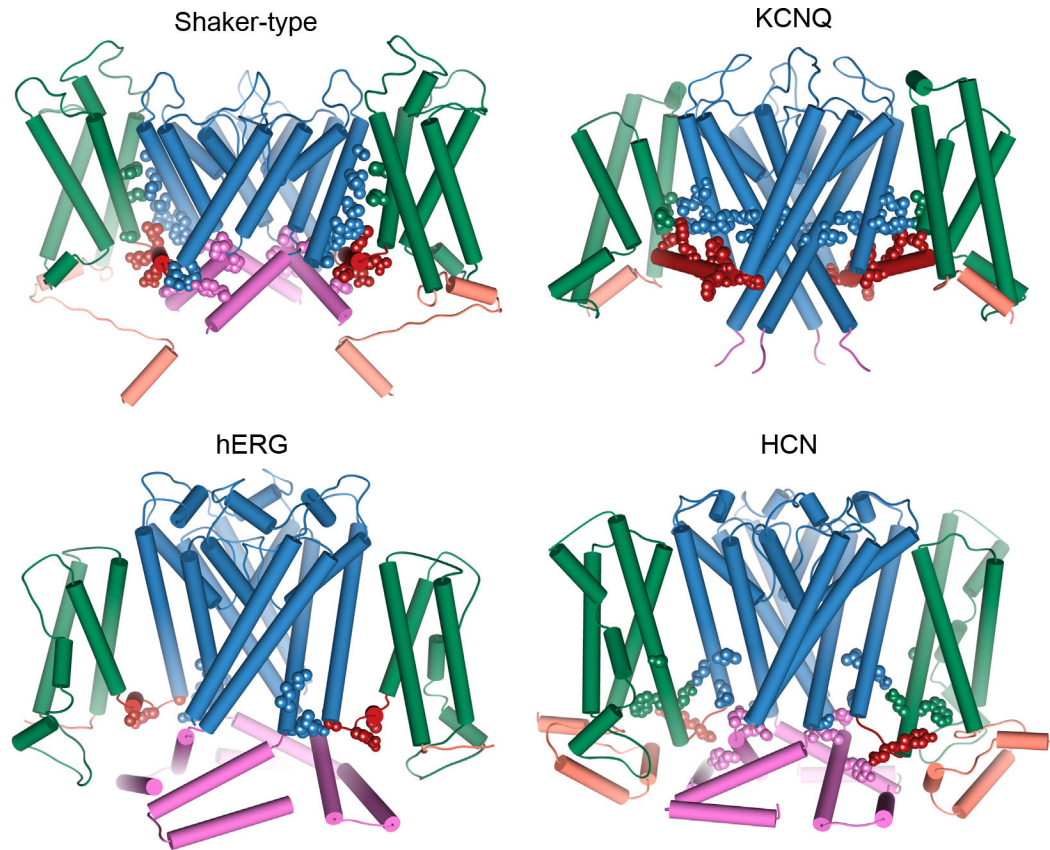


**Figure 5.** Comparison of the architecture and residues implicated in electromechanical coupling from several channel types. Shaker-type and KCNQ are domain-swapped while hERG and HCN are non-domain swapped. The N-terminus is colored in salmon, the VSD is in green, the S4-S5 linker is in red, the pore is in blue, and the C-terminus is in pink. Residues previously shown to be critical in coupling are shown as spheres colored according to the region they are found.